# Pleased or Petrified

An investigation of emotionally valenced stimuli and classification accuracy using functional magnetic resonance imaging

Maria Mujemula Olsen (202106384@post.au.dk) (MO)[1]
Sara Kjær Kristensen (202105320@post.au.dk) (SK)[1]

Supervisor: Line Kruse

**Cognitive Neuroscience**

**9th of June 2023**

School of Communication and Culture
Faculty of Arts, Aarhus University,
Jens Chr. Skous Vej 2, 8000 Aarhus, Denmark

June 2023

Characters: 49.690

Permission to publish: yes

[1] For individual assessment sections have been marked with a responsible author corresponding to one of the authors. It is stressed that this paper is produced in strong collaboration, meaning both authors contributed to most sections, the thoughts, and work behind.

## Abstract

This paper aimed to classify brain activity patterns for processing valenced stimuli using data from functional magnetic resonance imaging (fMRI) and training a support vector machine (SVM) and k-nearest neighbours (kNN) on the patterns. Literature review shows a different networks of brain areas for processing face, word stimulus and valenced stimulus. The fMRI method is compared, and applications and limitations are discussed. A study on 10 participants were conducted as a pseudo-forced two choice task where they had to categorize valenced or neutral word followed by a valenced face stimulus. The behavioural analysis shows significant difference in accuracy, such that participants were overall good at categorizing the stimuli. Results from first- and second level models on the fMRI data is presented and discussed. The classification model was made on different contrast maps then the rest of the analysis and compared the activation to a ground zero activation rather than baseline. A SVM and kNN model was trained on within participants and their accuracy was permuted compared to chance level. 3 out of 20 models showed significance. This method is thoroughly discussed, and alterations and improvements are discussed. We concluded the processing in the brain of valenced stimuli is a rather complex matter and we failed to make good classification models to find the contrasts.

# Table of Content

# Introduction (SK)

Facial expressions are one of the ultimate mediums of communication interlocutors can interpret. As it is thought to be a crafty tool for interpreting mental states and intentions, especially important in competition and collaboration (Heyes & Frith, 2014). Being able to recognize emotions in faces are of cultural (Boyd et al., 2011) and attentional importance attention (Schupp et al., 2006; Sutton & Lutz, 2019). The mind reading game is thought to be as much culturally learned as literacy. This paper will go down the rabbit hole of processing faces, emotions and words in the brain. As it dives into the recognition of negative and positive facial expressions using classification models on neuroimaging data from several participants. Firstly, we dig into emotional facial expressions.

## Notions on processing in the brain

### Emotional facial expressions (MO)

Humans ability to not only recognize faces but also the emotion recognition in faces (Holland et al., 2018) has been well established with the discovery of the fusiform face area (FFA) in the fusiform gyrus (first in (Kanwisher et al., 1997). The emotions later shown to participants were mediated in face like figures,  Different pathologies been identified like prosopagnosia, where patients have difficulty identifying faces associated with damage to extrastriate visual cortex  (Bear et al., 2016) page 362 and alexithymia, where patients have difficulty identifying and expressing emotions (Moriguchi et al., 2006) have.

Emotions have been discussed for decades. Modern belief supports Paul Ekman's six categories, which are thought to be universal across cultures: surprise, happiness, fear, sadness, anger and disgust (Ekman, 1992). The emotions were thought to be found in the limbic system (Maclean, 1949; Papez, 1937) comprising of the cingulate gyrus, temporal lope, amygdala and hippocampus. Contemporary discussions and research do challenge this categorical view on emotions and sectioning of emotions in the brain. For example, Hamann (2012) uses the valence/arousal scale for emotional categorization, such that emotions and emotionally valenced words can be mapped in a two dimensional space (see also Barrett (2006); Tsiourti et al. (2019)). Hamann argues that idea-to-area mapping like 'fear' mapping onto the amygdala is a stretch. As it has been shown that emotions are more network distributed and areas in the brain can play a role for several emotions as they are not limited to specific functionalities. In a broader view Ebner et al. (2018) showed that Caucasian people across ages and gender would rate emotional facial expressions using the handbook on five basic emotions (Ekman, 2000): happiness, fear, disgust, anger, sadness. And their own: neutral, excluding

surprise as it is often confounded with fear (Ebner et al., 2018). Results have showed that younger raters performed more accurately than older raters in identifying anger, disgust and sadness in faces; And that specifically across age groups happiness was the easiest recognized expression and then fearful and neutral faces in prioritized order (Ebner et al., 2010). The emotions later shown to participants were mediated in face like figures (see fig. 2 for example). For this study, participants do not only recognize emotional facial expressions, but they are primed with words.

### Semantic processing in the brain (SK)

When talking about words, we must talk about semantic and language processing. Just like emotion processing the language processing has become more complicated over the course of time. The contemporary model for processing language has been described by (Berwick et al., 2013) with two dorsal and a ventral pathway. Where the first dorsal pathway connects the superior temporal gyrus with Wernicke's and auditory areas to the premotor cortex. And a second dorsal pathway connecting from the superior temporal gyrus to Broca's area. Lastly a ventral stream from Broca's area to the auditory cortex. All of these pathways are thought to speech production, processing complex syntactic structure and abstracting meanings from sound respectively (Bear et al., 2016, p. 694). These parallel language pathways seem distinct but according to theory they also interact with one another (fig 1).

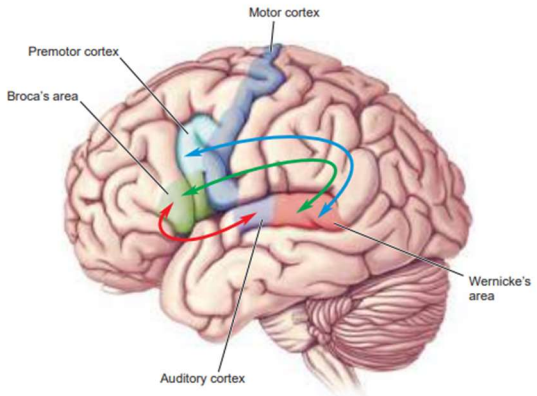


*Figure 1 - copyright Bear et al., 2016, p. 704*

Posner & Raichle (1994) showed interesting results using PET to pinpoint activation areas when seeing, hearing, speaking and generating words. Following the parallel language pathways, they found "seeing words" showed activation in striate and extrastiate cortex corresponding to visual processing theory. Just like faces have the FFA, words seem to have their own recognition area in the fusiform gyrus called the visual word form area (Mahon, 2022).

Reading a word is most likely to be within a context either provided by the surrounding words or the patches of prior experience with the word via top-down processing. Rarely a word is

read without any meaning attached to it. (Xu et al., 2017) carefully investigated valanced words using (Binder et al., 2016) labels and categorizations. They proposed neural networks translating the semantic processing to language production and comprehension: default-mode-network (DMN), perisylvian network (PSN) and left frontoparietal network (IFPN). A tri-network for semantic tasks, selective attention to sentences over nonwords and multi-demanding system of sensorimotor-related control and conceptual domains respectively. This meta-analysis underlines the point that language and semantics are complex yet systematic.

### Systems (SK)

For one the amygdala has got a lot of attention for having a fast track when processing negative, fearful or threatening stimuli. (LeDoux, 1996, 2003) calls it the fast response of e.g., visual stimuli processing through the visual thalamus and then the amygdala rather than processing thoroughly through the visual cortex first. Such that the sympathetic nervous system can react instinctively in fight or flight scenarios. This fast track is also somewhat questioned as to amygdala's emotional selectivity might not be as definite (Ward, 2020). The same kind of fast track has not been put together for positive stimuli, as positive emotional neural networks are thought to be widely distributed rather than centralized (Ward, 2020).

How emotional facial expressions and language is processed seem to become more and more complex the more we learn about them. The information era like to think of the brain as a computer with well described networks. With modern technology we can get closer to these complex structures as this paper will investigate brain activity with different valanced stimuli using functionality of magnetic resonance imaging (fMRI). We will take a step can into neurobiology before stepping into the fMRI methodology.

## Neuroimaging

### The measure of the activation potential (MO)

In order to understand how brain activity can be measured, it is necessary to understand the mechanisms of neurochemical signalling. Neurochemical signalling is caused by an activation potential, which refers to the depolarization of a neuron's membrane due to a positive change in charge within the cell (Gazzaniga et al., 2014). The resting potential of a neuron lies at approx. -70mV. The resting potential is maintained by sodium-potassium ion-gated pumps. These ion-gates keep the intracellular space negatively charged relative to the extracellular space by actively pumping Na+ ions out of the cell and K+ ions into the cell (Gazzaniga et al., 2014). When the intracellular charge reaches approx.

-55 mV in the trigger area, which is at the part of the axon closest to the soma, the Na+ pumps open, allowing Na+ ions from the extracellular space to enter the neuron causing a depolarization. This in turn prompts the opening of K+ pumps, resulting K+ ions flowing from the neuron's cytoplasm to the extracellular space, thereby repolarizing the neuron. The change in charge activates neighbouring Na+ pumps, causing the signal to travel down the axon. Due to a brief period of hyperpolarization, the signal cannot travel backwards on the axon, leading to unidirectional signalling that terminates at the terminal end. Neurotransmitters are then released to the synaptic gap, either facilitation or inhibiting the signal in the post synaptic neuron.

This process forms the basis of neuronal communication, and activation potentials are crucial for brain functioning. Sodium-potassium ion-gated pumps therefore play a vital role in electrical signalling. Since both Na+ and K+ travel against the concentration gradient, the sodium-potassium ion-gated pumps require energy in the form of ATP to function (Gazzaniga et al., 2014). For the mitochondria of a cell to produce ATP for these pumps, the cell requires oxygen, which it extracts from haemoglobin in the bloodstream. Following the firing of an action potential, the ion-gated pumps work more vigorously to re-establish the resting potential. This increased activity demands more energy, resulting in increased blood flow to the active area of the brain. This fact is used in several different methods to infer brain activity related to the exposed environment.

### The methods of inferring brain activity (SK)

When studying the effects of human behaviour, the goal is to understand and explain as much of the behaviour as possible. However, relying solely on behavioural data, such as choice and reaction time, has its limitations. To gain further insight into the underlying mechanisms of specific behaviour, it is valuable to complement behavioural data with information about brain activity.

Techniques like single cell recording offer high spatial and temporal resolution, which can provide valuable information about specific behaviours. However, obvious ethical considerations often lead to the preference for non-invasive methods such as electroencephalogram (EEG) and fMRI when investigating cognitive processes related to behaviour. EEG has high temporal resolution but poor spatial resolution, whereas fMRI provides higher spatial resolution but relatively poorer temporal resolution for the flow of activation potentials. Therefore, the choice of methods depends on the desired information to be combined with the behavioural data. Another substantial difference is that no harm will come to the patient during EEG and fMRI studies, whereas single cell and positron emission tomography (PET) are more invasive and will potentially leave marks.

The primary focus of this study is to gain deeper insight into the brain regions activated during the processing of emotional facial expressions. Hence, fMRI is chosen as it can provide better spatial resolution, which aligns with the study's objectives.

### FMRI (MO)

Unlike EEG, fMRI does not directly measure the electric flow of action potentials, but rather oxygenated blood. Since fMRI assumes that active brain regions will have a higher concentration of oxygen due to the increased blood flow in the area as well as there being a higher concentration of oxygen molecules because more oxygen will be supplied than the neurons need compared to a baseline state of flow (Amaro & Barker, 2006). The oxygen is a key player since the ferrous irons bounded to the haemoglobin structure contributes to the blood flow's magnetic properties (Goldstein & Van Hoff, 2020). In areas of high activity, the oxygen will be distributed to the working environment, converting the oxyhaemoglobin into deoxyhaemoglobin as described in section above. During this process the properties of the magnetic field changes slightly. This alters the magnetic susceptibility of the blood enough for a 3-tesla magnetic field to pick up on it, and thus makes it possible for measurement (Buxton, 2013). The oxygen level in the blood is expected to be higher in active brain regions due to the need for oxygen in the process of making energy in the form of ATP (Amaro & Barker, 2006). The signal measured in fMRI is therefore called the Blood Oxygenated Level Dependent signal (BOLD). Since the blood flow is slightly delayed, the peak will first arrive about 4-6 seconds post stimulation and can last up to 10 seconds (Huettel et al., 2009). The overall difference in BOLD is usually under 10 percent compared to baseline (Schölvinck et al., 2008).

To further understand fMRI, we will take a closer look into the mechanisms of image acquisition. The magnetic field in a MR scanner uses the fact that free protons, primarily found in the body as hydrogen protons, can align themselves in response to a strong magnetic field. The protons' spin around the magnetic field aligns at a specific frequency called the Larmor frequency. The aligned protons' spin can be changed by pulsing radiofrequencies so that their magnetic moments are perpendicular to the main magnetic field. When the protons return to their original spin orientation after the radiofrequency has ceased, a radiofrequency voltage is emitted, and this is what is detected by a gradient coil (Bear et al., 2016, p. 189). During this process two types of these signals occur: Type one (T1) involves realignment of the protons to the magnetic field while Type two (T2) refers to the dephasing of spinning protons or loss of resonance (*MRI Interpretation*, n.d.). T1 signals highlight differences in tissue based on the speed of realignment. A faster realignment is equal to a greater T1 signal. The T2 signal captures the proton dephasing, where a slower dephasing means a greater signal.

Due to differences in proton behaviour in different tissues, T1-weighted images are useful for highlighting fatty tissues, as protons in fat realign quicker while T2-wieghted images are effective for distinguishing watery tissues. Using an echo gradient based on the magnetic gradient to generate a signal rather than a radiofrequency pulse, means we can acquire images faster (Hargreaves, 2012). These weighted images are in other words sliced images of the brain in three dimensions, that combined visualizes the brain in a three-dimensional image consisting of general values of radiofrequencies from small cubes in the brain, voxels. Usually, the number of voxels per image is set to 250x250x50 resulting in 3,125,000 voxels. One generalized value is assigned for each voxel over a specifies timeset. From this information it is possible to model the expected BOLD signal over time, which can be used to identify and measure if specific areas of the brain are active at certain events. Making it possible to compare different events activation pattern.

### Choice of algorithms (SK)

In this study we wish to go a step further, as we want to explore the possibility of prediction of behaviour/stimuli based on previous activated areas. In order to do this, a machine learning approach will be utilized by training a classifier on neuroimaging data. This method is often referred to as Multi-Voxel Pattern Analysis (MVPA) (Mahmoudi et al., 2012). MVPA has three steps: feature extraction, which converts the BOLD values into relevant variables for classification; feature selection, where the relevant variables are cut down to improve classification; cross-validation to test algorithm on unknown data and determine accuracy of classifier (Al-Zubaidi et al., 2019). Patterns can be classified by classification algorithms trained on unique subset of the original dataset and later tested on the remaining of the original dataset. This way the classification accuracy is solely tested on unknown data, as there is no leak of data between the training and testing dataset. The classification accuracy is commonly compared to other algorithms performance or to chance level, in order to say whether the algorithm performed better than chance or the algorithm to classify the unknown data into the correct groups. The algorithms used for machine learning classification can either be supervised or unsupervised in order to find patterns depending on prelabelled training data or not. In this study supervised machine learning will be used.

### Classifying (MO)

Algorithms come in many shapes and sizes for different needs. Common algorithms used in supervised machine learning are linear regression, decision trees, random forests, k-nearest neighbours (kNN) or support vector machines (SVM). As SVM and kNN will be used in the analysis of this paper, only these will be elaborated upon for the sake of simplicity.

Starting out SVM was introduced by (Cortes & Vapnik, 1995) with the assumptions of dependency in binomial data. Which is a great advantage for fMRI and cognitive processing as it is in general processed somewhat serial and conditional. Take retinotopy as example of serial processing for visual sensory processing (Bear et al., 2016). There are several kinds of SVM's, but what calls for all of them is that SVM maps the datapoints in a dimensional space, where dimensions correspond to different classes of the data. A hyperplane is then fitted to accommodate as many datapoints as possible (Cortes & Vapnik, 1995). The simplest way to fit the hyperplane is to make a linear classification. In regression language, this means to draw a three-dimensional space while saying "high-dimensional", plot the data according to its groups - the dimensions - draw a straight line - the hyperplane - through the space, while trying to keep the groups apart. Such that whatever is above this line is probable to be in group A and whatever is below this line is probable to be in group B. Here above and below are arbitrary chosen to paint the picture of differentiating two groups from one another. Meaning that training a linear SVM is to learn a model how to draw the best straight line through a high-dimensional space on labelled data.

But fMRI data is all about voxels and areas, so what activation pattern the neighbouring voxels has would most likely influence or at least also be predictive of the activation in this point of view voxel. Introducing kNN first introduced by (Altman, 1992). This algorithm assumes the data to be dependent because of the proximity to other datapoints in the same group. Much like SVM, kNN will try to classify the data's group labels, but by checking the surrounding number of voxels (k) rather than what side of a hyperplane the point is on. The k can then define the size of the search area, such that the algorithms decision is based on the entire town of data of just the single one-way street, where the data 'belongs'.

For both algorithm the testing phase includes them giving their most informed guess based on what they have learned from the training data. The output of this test is a permutation accuracy to describe how well the algorithm performed on the shuffled unknown testing data. Based on what we now so far, we formulate a hypothesis.

## Hypothesis (SK)

We hypothesis that voxel activation patterns across participants will cluster in brain areas related to emotional and semantic processing as well as in the visual cortex when participants shown images of negative and positive faces.

With such complex systems to process semantics yet such specialised networks in face and word recognition, we hypothesis that we can train classification models to correctly identify when a participant is seeing a positive or negative face. Based on the theory about the classification algorithms we would expect the kNN to perform better than the SVM, since it understands the importance of location.

## Experimental setup (MO)

To address these hypotheses, we first conduct an experiment with fellow students as follows.

### Participants (MO)

10 cognitive science students voluntarily participated in both a pre-scan and in the following study. The participants were informed of potential risks and warnings when signing up for the study and everyone had to pass a pre-scan to participate in the study. Of the 10 participants 7 were female and 3 male, age 20-24 (mean = 21.7, SD = 1.4). The study was conducted by the participant's fellow students and teachers in groups of about 5 students and one teacher.

### Setup (SK)

Two scanners, a Skyra MR scanner and a Prisma Fit MR-scanner, were used for data collection loca ted at Aarhus University hospital. All scans were conducted throughout the course of five weekdays with a study before and after 12 o'clock. It holds for both scanners; that a standard head coil was us ed, the scanners obtained both T2-weighted echo-planar images (EPI), with BOLD contrast and T1 weighted structural images. The anatomical images were obtained in the dimensions of 176x256x25 6 voxels (XxYxZ dimensions) with a voxel size of 2,7x2,7x2,97 $mm^3$. The functional images were i n 76x76x45 voxel dimensions with 610 timepoints. Each voxel was about 2.5x2.5x3.0 $mm^3$ with a s ampling rate of one second. Each MR-scanner held a monitor with the dimensions of 1200x1000 pix els and a frame rate of 60 hz.

### Stimuli (MO)

This study relies on material from the (Binder et al., 2016) paper where they have rated many words. The binder et al. found 65 semantic features which are argued to have neurologically distinguishable functional representations. That is cool but we are interested in negative and positively valence so for this experiment each word had a calculated word score based on a principal component analysis with four of the semantic features ("pleasant, unpleasant, happy and sad"). Each label is then validated by

comparing to the Warriner sentiment database (Warriner et al., 2013), such that word scores > 6 are labelled positive, <5 labelled negative and everything in between is labelled neutral.

For each participant 360 words are randomly selected from the word scores, so each label is represented the same number of times. The 360 words were categorized into sessions, such that no words appeared more than once per participant. The second half of the experiment was the facial expressions. Through the experiment participants only ever saw faces identical to the faces in figure 3.

### Procedure (SK)

The task for this study used a pseudo two-alternative forced choice task with a passive followed by an active component. The experiment was run in 6 sessions of 10 minutes duration. To ensure comfortability for the participants, a break was offered between each session. After being presented with a word either positive, negative or neutral for 700 ms each participant was shown a face either negative or positive and was asked to make a choice. The delay between the two components varied from 3-5,6 seconds with a mean of 4,1 seconds in order to enhance the unpredictability in the trials to increase the likelihood of the participants responding according to protocol rather than just waiting for the face to be shown. With a 2-button response pad, the participant was asked to respond with either index finger for “positive response” on a blue button or with middle finger for “negative response” on a yellow button whether the face was positive or negative. The button pad was placed in the participant’s dominant hand. It should be noted that each positive and negative valenced words is always followed with a positive or negative face respectively. The neutral words are randomly assigned an emotional face. An example of the experimental walkthrough would go as follows:

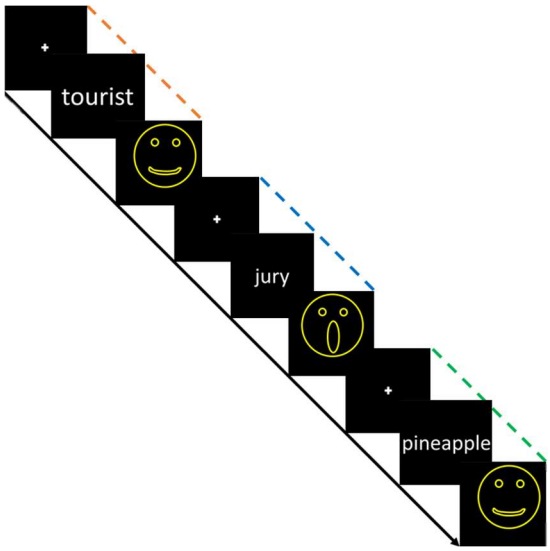


*Figure 2 - Example of experiment trials in zoomed version for explanations sake. Orange: neutral word + positive face = neutral trial, blue: negative word and face, green: positive word and face.*

## Statistics[2]

### Pre-processing (MO)

The BOLD images obtained from the fMRI scanner underwent pre-processing steps. This consisted of skull stripping and segmentation. Furthermore, the BOLD images were slice time corrected for acquisition order and were also realigned to a T1 image and each other to correct for motion artefacts. The data was also spatially normalized to the Montreal Neurological Institute (MNI) brain average. Lastly, the data was also head-motion corrected.

### First and second level models (MO)

A first level analysis was conducted on the pre-processed BOLD images in a Brain Imaging Data Structure (BIDS) using Jupyter Notebook version 3.3.2 (Kluyver et al., 2016) with Python version 3.9.10 (Van Rossum & Drake, 2009) on UCloud. The Nilearn package (Abraham et al., 2014) was utilized during the analysis of the BIDS data.

The first level model objects were obtained and model desired confounds were specified. Design matrices were created for each run pr. participant containing 5 columns with expected HRF-convolved timeseries given the condition of the stimuli, six rigid body transformation

[2] All computations and code snippets are to be found in Sara's member file for cognitive neuroscience ucloud course for scripts on UCloud in the 'exam' folder.

parameters (three rotations and three translations), three global signals (global signal, cerebral spinal fluid signal and white matter signal), as well as 12 cosine regressors (drift parameters) as a method of high-pass filtering to account for low frequency parts in the data. An example of such a matrix is displayed below.

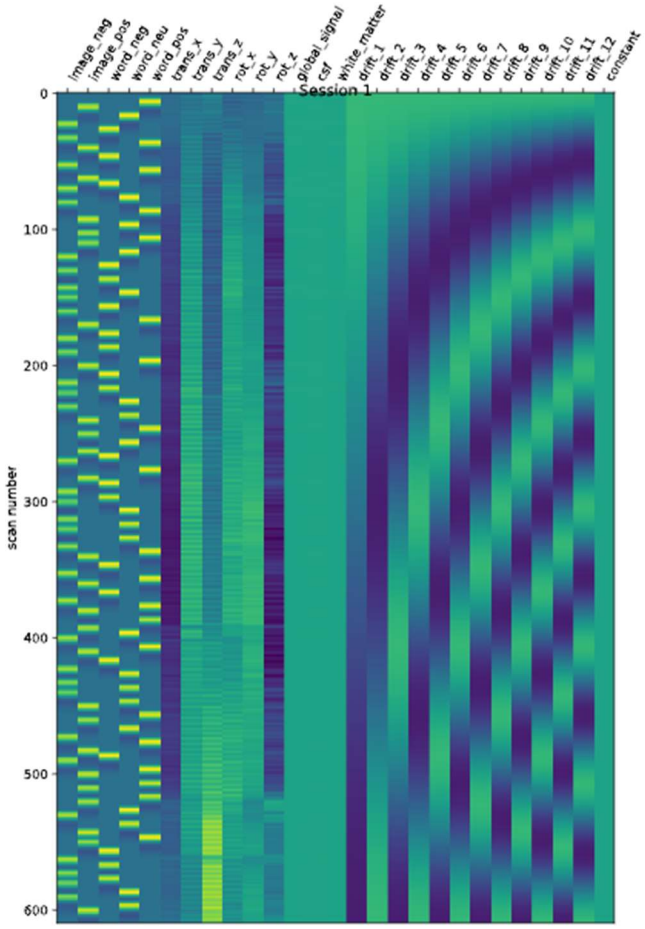


*Figure 3 - Design matrix for one participant's first session*

Two contrasts where created, namely image_neg-baseline and image_pos-baseline, to investigate significant differences in voxel activation in these conditions and the baseline signal. The data was then modelled by fitting it to the defined design matrices and thereby estimating the fMRI response for each condition and participant. To assess statistical significance of the contrasts, z-maps were generated for each of the six sessions and for both conditions per participant. An uncorrected p-value threshold for statistical significance was set to $p<0.001$.

A second level intercept model was then fitted to the z-maps for all participants for each of the two conditions in order to investigate activation patterns on a group level. A spatial smoothing kernel of 8mm was applied in the second level analysis.

In order to account for false positives in multiple hypothesis testing, Family-wise Error Rate (FWER) correction was conducted on the z-maps applying non-parametric permutation tests as the FWER method (Fisher, 1971; Pitman, 1937). The effects are now negative log of the p-value. A brain atlas on the results from the second level model was then conducted using the Atlasreader package (Notter et al., 2019) in order to gain more information on activation voxel clusters.

### Classification (SK)

A classification model was then made on the BOLD images in order to investigate whether a model could successfully classify if a participant had been shown a positive or a negative image based on voxel activation patterns. Everything was run individually, meaning first level models were conducted on each participant for the classification model, since people's brains are assumed to be different at least in size and therefor in area positioning.

A similar process as the one described in the previous section was applied for obtaining the first level models. However, the models were fitted to a design matrix that produced one beta estimate for each trail rather than pr. condition.

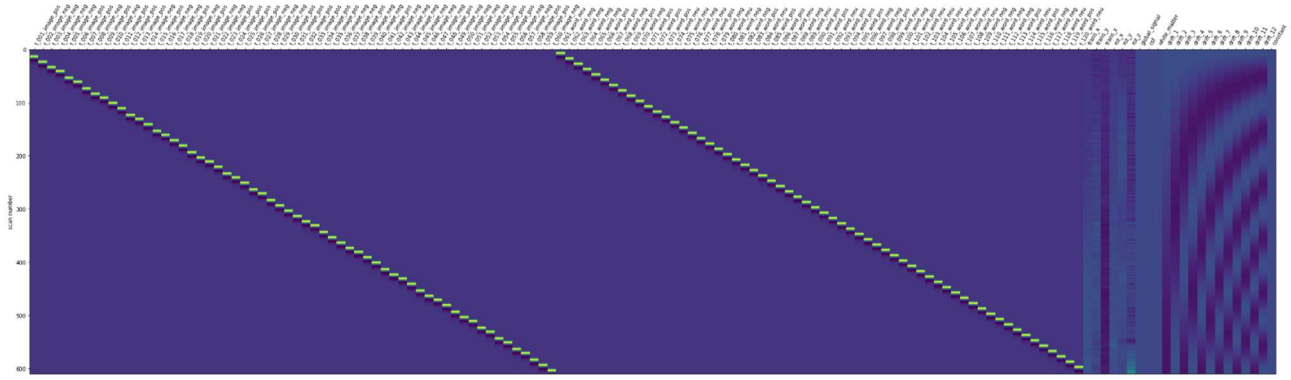

*Figure 4 - design matrix for one participant for one session with one beta estimate for each trial.*

The data was then modelled by fitting it to the image trails, as this is what we are investigating, in the design matrix. Z-maps were then created for each participant for each session based on contrast defined as each trial compared to the baseline. The data was then reshaped so that the trials were paired with their condition label. This was done in order to run supervised machine learning as will be described further down.

As the last pre-processing step, we create brain masks for each participant, where we specify that we are only interested in voxels in the z-dimension interval [30:160], meaning that any data of any kind outside of this range is discarded. The areas described in the literature review should mostly be included in theses slices as it is mostly the cerebellum. We do this to gain time in our

computational resources, well knowing we are losing some data. We argue this is a safe choice for the scope of this paper. We then split the data into 80% training data an 20% test data to avoid data leakage.

Two classification models, one for Support Vector Machine (SVM) and one for k-nearest neighbours (kNN), where set up using Nilearn's Searchlight function (Etzel et al., 2013). For both types of models apply that the parameters were set to a radius of 5 mm to check for powerful predictive voxels and cross validation folds of 3 with a verbosity level of 10. kNN had an additional argument of looking at the three nearest neighbours. These arguments could have been even more precise. However, the mentioned arguments were set due to limited computational power.

After fitting each searchlight module for each individual, the 500 most predictive voxels were found, and the processed masks were updated before moving on to permutation testing. The permutation test is to assess our trained model's accuracy on unseen data. This is where our second split of data comes in, the testing data. Each model is as said before trained using either linear SVM or kNN, but trained on each participants own data. As follows the testing data will be the second split of each participants data.

# Results

## Behavioural (SK)

We use R (R Core Team, 2022) and Rstudio (Posit team, 2023) to plot using tidyverse (Wickham et al., 2019) to firstly investigate the behavioural data. One participant's behavioural data was lost, therefor only 9 participants are depicted. The mean response time was 0.64 seconds with a standard deviation of 0.15 seconds. Here plotted as response time across trials with the mean represented as the black bar and the grey bars the 96% confidence interval:

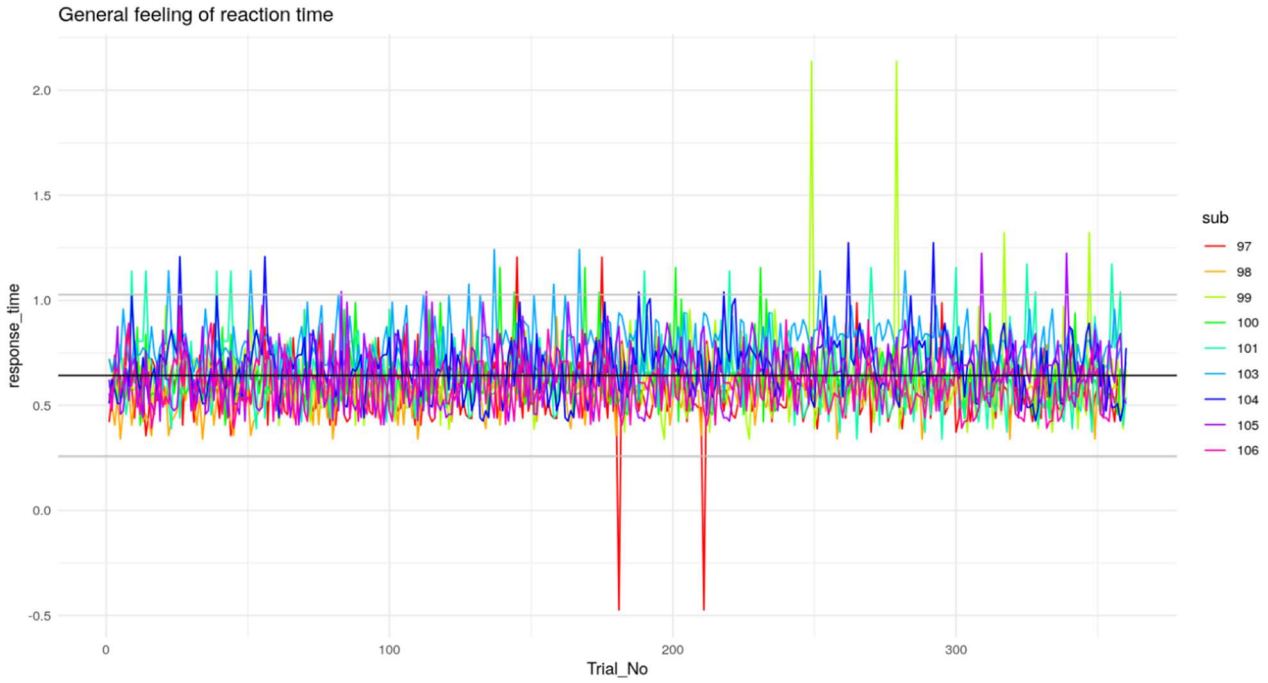


*Figure 5 - response time across trials, the order of words and trial types were mixed for participants.*

Both response buttons were used almost the same number of times (1643 for positive and 1588 times for negative). The participants were overall very accurate in their ratings with 417 wrong responses and 2814 accurate response. This is a statistically significant difference when a one sampled t-test is conducted ($p < 0.05$). Here we see the pattern of correct response across trial types:

Accuracy across trial types

| Accuracy\Trial type | Face Neg | Word Neg | Face Neg | Word Neu | Face Pos | Word Neu | Face Pos | Word Pos |
|---|---|---|---|---|---|---|---|---|
| False | 135 | | 91 | | 65 | | 126 | |
| True | 941 | | 456 | | 467 | | 905 | |

*Table 1 - distribution of accurate responses across trial types. Where 'false' means wrong answer and 'true' mean correct answer.*

## First- and second level models (MO)

Figure X displays first level z-maps for each condition pr participant for session 1 (note that z-maps for each session was created), with higher positive or negative z-scores indicating more pronounced activation or deactivation respectively. The activation patterns seem to be somewhat random. However, there seems to be more clustered activation in VI for most participants, and perhaps slightly higher activation in the image_pos condition. Furthermore, higher activation also seems to occur in the somatosensory cortex across participants.

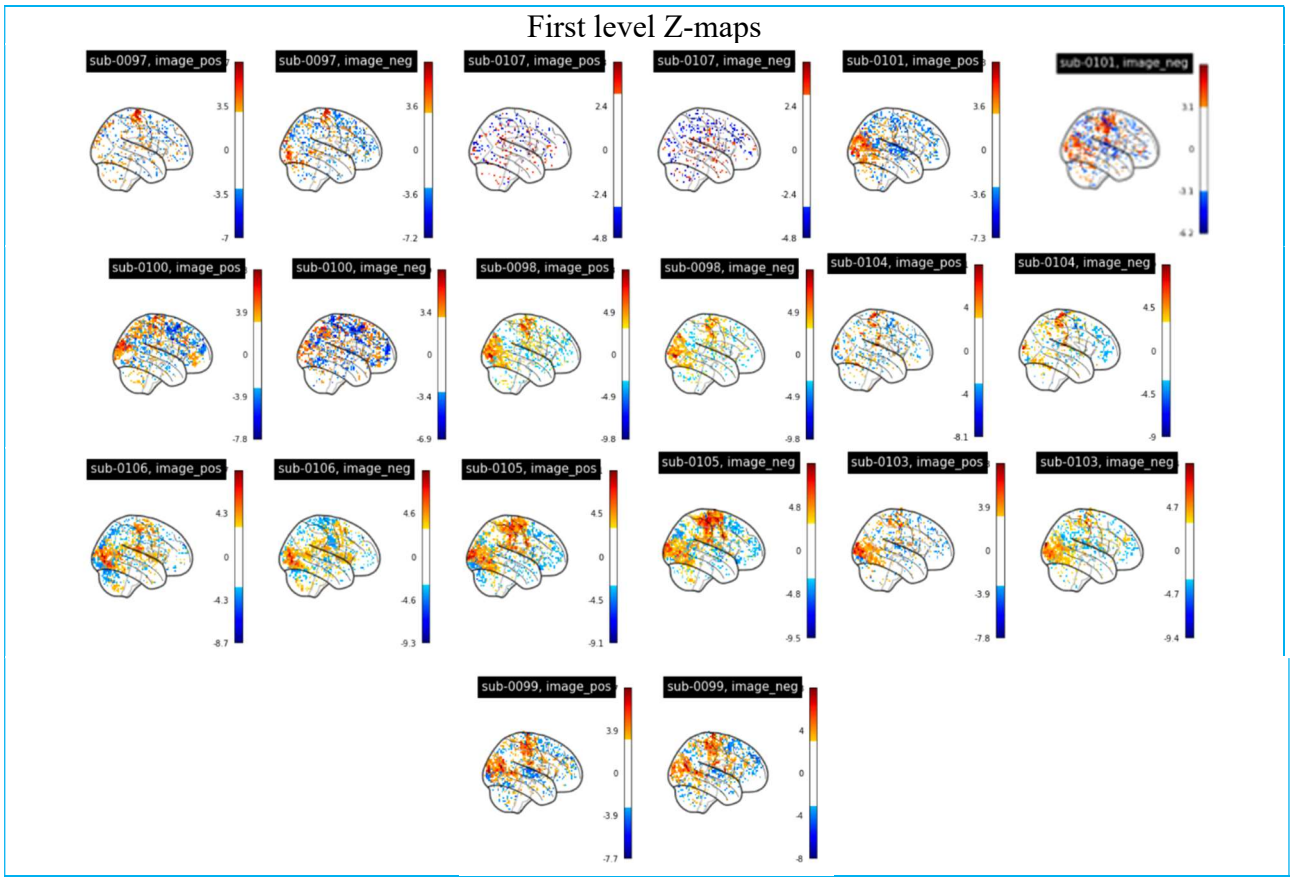


*Figure 6 - z-maps for each of the 10 participants, 2 z-maps pr. Participant, one for each condition*

In order to gain a quick overview of activation patterns, we take a closer look at the second level model z-maps for positive image and the negative image conditions, with uncorrected p-value threshold, which are displayed in figure 7. There seems to be higher activation in the occipital lobe as well as the primary somatosensory cortex for both conditions, with a slightly higher activation overall in the negative condition. Furthermore, there seems to be less activation than in the frontal lobe:

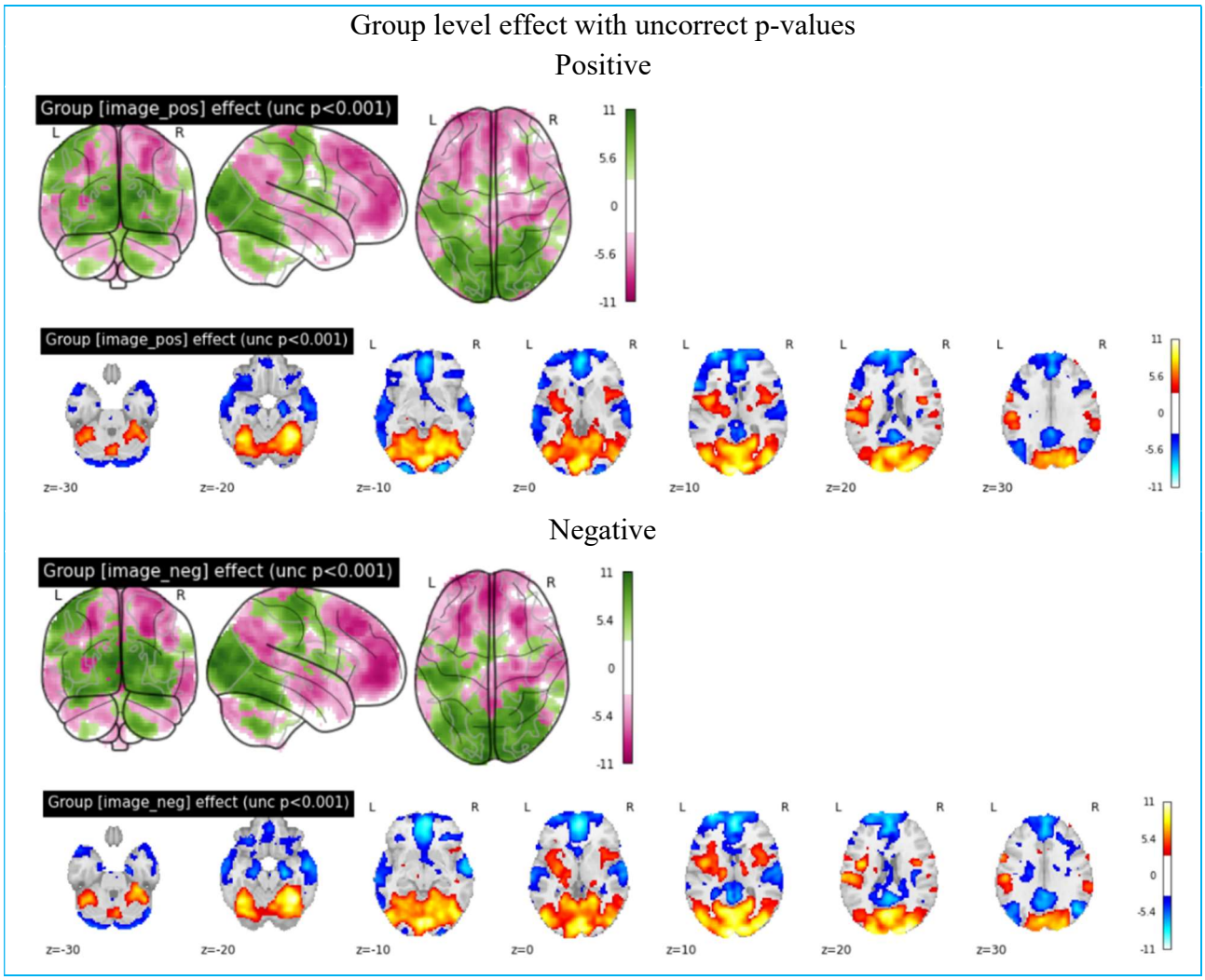


*Figure 7 - Second level model z-maps with uncorrected p-value thresholds generalized over all 10 participants within image condition*

The second level z-map with a corrected p-value from the permutation test is displayed in figure 8. There seems to be much less difference in activation from the baseline overall, which is likely due to the reduction of false positives in voxel activation. However, there still seems to be higher activation in the occipital lobe and the primary somatosensory cortex for both conditions as seen in the z-maps with uncorrected p-values.

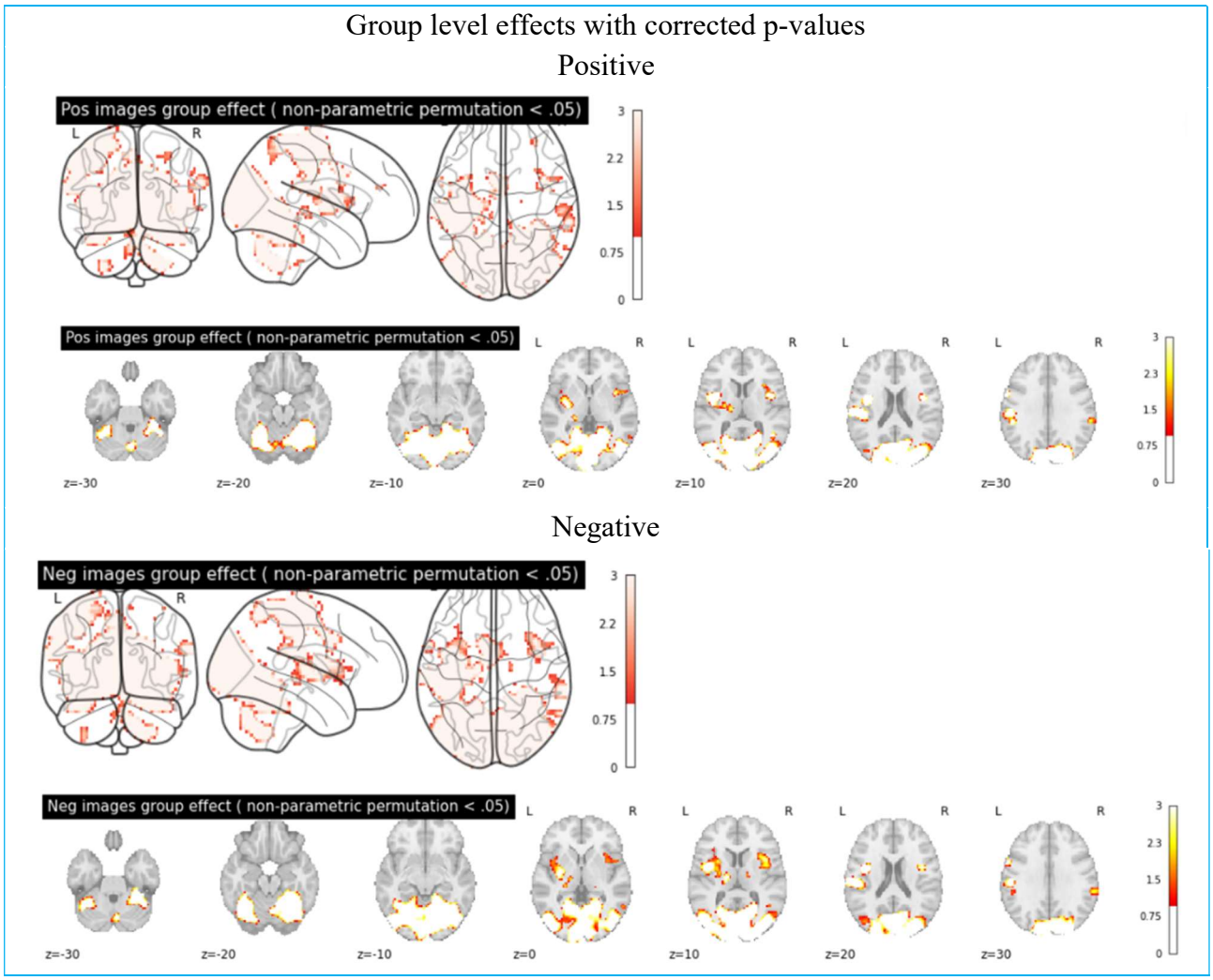


*Figure 8 - Second level z-maps over all participants within image conditions with correct p-values obtained by non-parametric permutation with a threshold of <0.05.*

Taking a closer look which areas of the brain there appear voxel activation clusters, the model output of the atlas maps was examined. (See table 2). Activation occurred in similar brain areas for both conditions. In both conditions the activation clusters occur in the lingual gyrus, which is in accordance with semantic processing, as well as in the singular gyrus, which is part of the limbic system and amongst other things is involved in emotional processing. Furthermore, the postcentral gyrus, involved in somatosensory processing as well as motor control, is activated in both conditions:

| Top activation areas for the two conditions | | | |
|---|---|---|---|
| Comparable | | | |
| Name | Size positive | Size negative | |
| Right supramarginal gyrus posterior | 2521,64 | 2250 | |
| Left insula cortex | 8961,63 | 10028,40 | |
| Left lingual gyrus | 199152 | 205436 | |
| Left singulate gyrus | 4112,22 | 6459,29 | |
| Left postcentral gyrus | 41742 | 42033,90 | |
| Positive | | Negative | |
| Name | Size | Name | Size |
| Right insula cortex | 3704,89 | Left thalamus | 2114,30 |
| Left cerebellum cortex | 1512 | | |

*Table 2 - sizes are always in $mm^3$ and all areas have a peak value of 3.0.*

## Classification (SK)

For our SVM and kNN classification models. We see our models' performances of accuracy is almost coin tosses rather than informed guesses. The kNN models have a permutation accuracy ranging from 0.43-0.62 (mean = 0.53, SD = 0.06) with p-values of accuracy in the range 0.03-0.83 (mean = 0.41, SD = 0.28), whereas the SVM models have a permutation accuracy ranging from 0.41-0.64 with same mean and standard deviation with p-values of accuracy in the range 0.03-0.9 (mean = 0.38, SD = 0.28).Which we all in all summarize in the plot below.

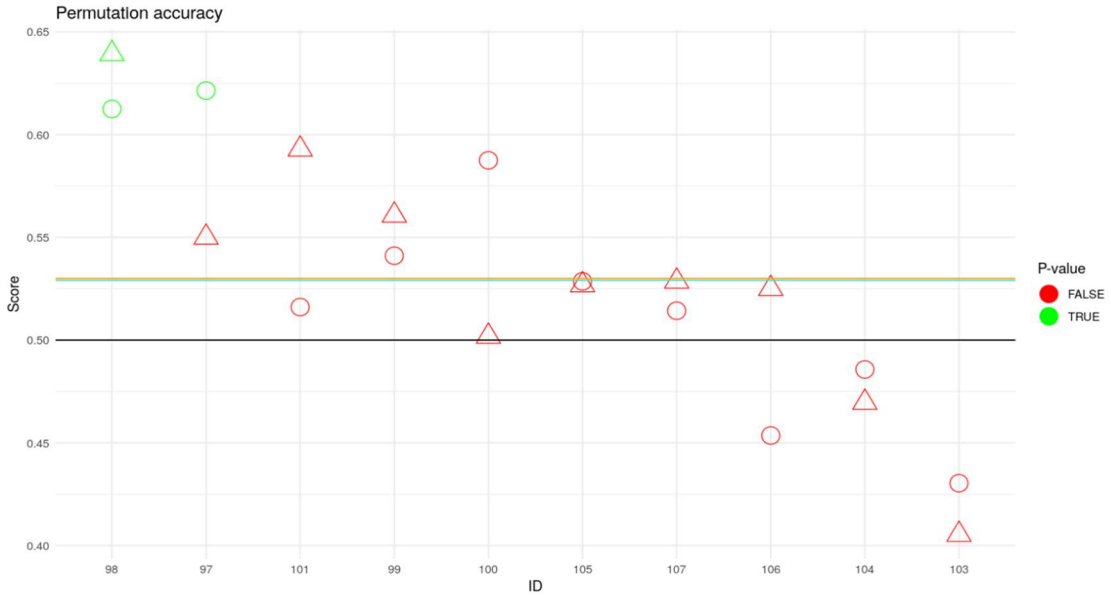


*Figure 9 - Round is kNN and triangle is SVM, orange line is SVM's mean, blue line is kNN's mean, black line is chance level. The plot shows each participant's models and accuracy on the test data and the colour scale represents the p-value. True means below 0.05 and red means above.*

Lastly, we take a look at the contrast maps 500 most predictive voxels and their whereabouts.

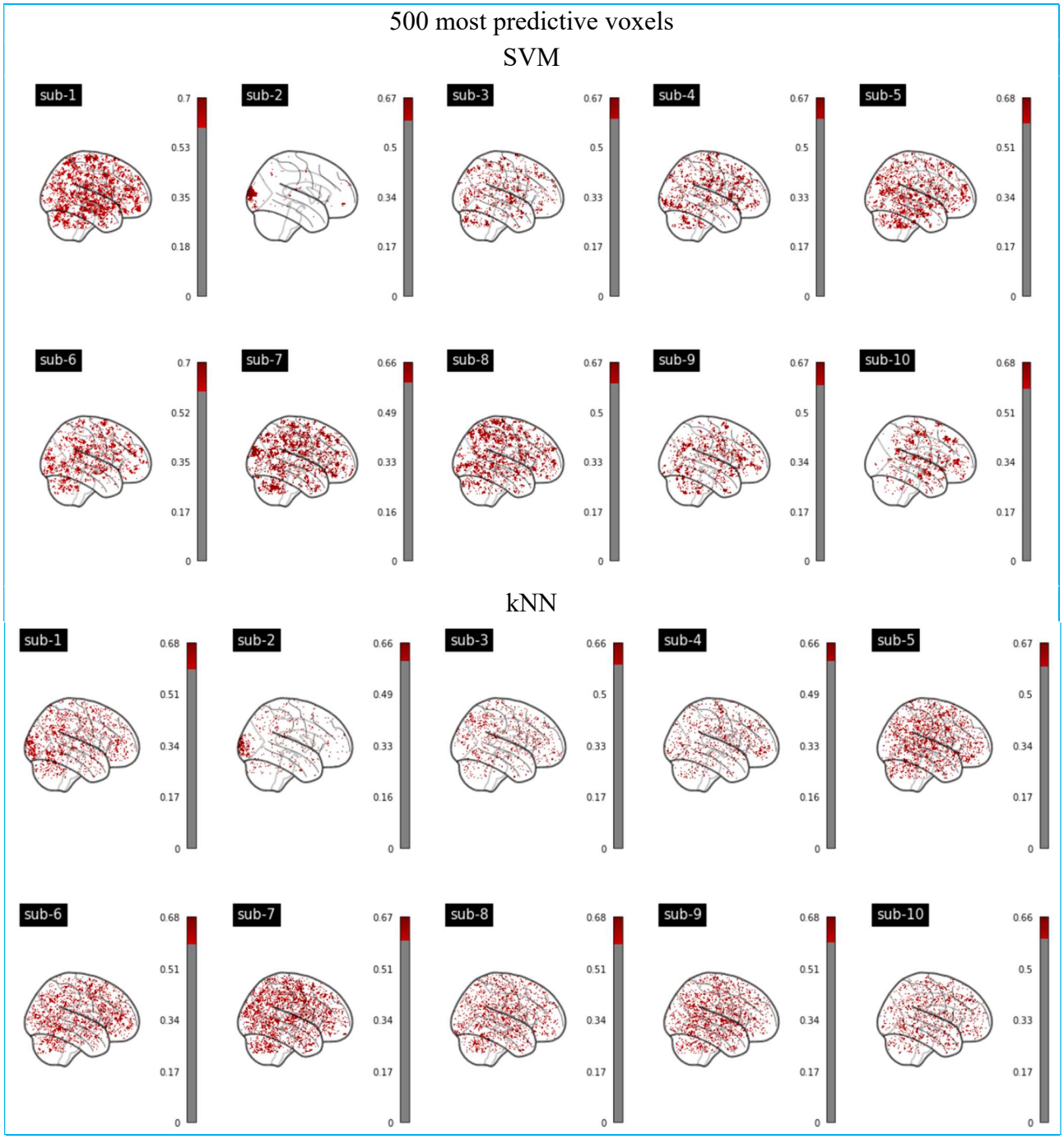


*Figure 10 - classification accuracy of the individually trained and tested models. The red is to indicate voxels with accuracy above 0.06.*

As these patterns visually appear to be widely spread and individual, we will not comment on the areas the voxels are found in.

# Discussion

## Results

*First- and second-level models (MO)*

From the results of the second level models, there seems to be evidence for our first hypothesis, as voxel cluster activation mostly found areas align with the literature as it is a visual task where faces and words are decoded in an fMRI where the participant is trying to keep still (primary somatosensory cortex). This aligns fine with the pattern of V1 and primary somatosensory cortex, since it follows the literature on what processing goes on where (Meadows, 2011; Raju & Tadi, 2023). Yet the insula is in top six of contrast areas, which is fairly interesting since emotion research adores the insula for dealing with taste and most often the feeling of "disgust" (Ward, 2020). These results are somewhat compatible with previous findings from the same procedure and study (Fyhn Sørensen, 2022). Reasons for this is probably because of the irregularity of our experimental task or the population size. As we have added these findings to the previous year's results, we see we either need a lot more data or we are close enough to where would end up if we had infinite amount of data.

We also did not look at contrasts for the different words, which could be interesting to investigate as the words act as a primer for the following face. Such that we could add to the model whether the participant classified the neutral words as negative or positive. Yet the participants still do not have to pay much attention to the word as their response is asked to be after the face stimuli, such that they could just wait for the face stimulus to appear before answering.

*Permutation (SK)*

The 500 most predictive voxels appear to be wildly spread. It is impressive that it then could significantly classify for 1 participant as the difference is hard to tell (Schölvinck et al., 2008). As our models perform slightly better than chance, we really cannot use the models for much. We cannot accommodate our hypothesis about either SVM or kNN models to perform well neither that kNN outperforms SVM. One reason for the poor performance of the classification model could be explained by there not existing a difference in voxel activation patterns between the two image conditions. This at least also seems to be the case based on the second level analysis showing very similar activation patterns for participants when shown a positive or a negative face. However, adding more predictors or fitting the same model to the entire group would probably be a good idea to make the classification models train on more data on even more informed guesses (Smaldino, 2017). This would also allow for more generalizable results for the future to use, as it would be trained on multiple people rather than one

specific person at the time, whose energy or processing might be slightly different from others. This use would also be preferred in clinical settings for aiding diagnosis of different psychiatric and cognitive disorders if such patterns could be generalized from several patients and controls.

A whole other approach would be to make the 4D images of the brain activity into 2D images and then running an image classification of the different images for the different trial types. Some of the beauty of the fMRI data is lost, however that is how it is when you want to generalize. If the model is too specific it underfits, if it is too poorly informed it overfits. Finding the sweet spot can be hard, especially when one is looking for a pattern in randomness.

As going forward, it would be interesting to test the model on completely new data, that it had not even seen the anatomy of yet to really test the model's accuracy. This means in the meantime that our results from the permutation tests are rather arbitrary as it does not take the baseline or difference of conditions into account. Colleagues of the authors did somewhat the same classification pipeline, yet they generalized the conditions contrast z-maps before classifying. Giving the models a limited number of z-maps to train and test. This method could be on to something, yet the pattern recognition of the model is discarded as the model ever sees the mean activation pattern for the different conditions and still does generalize across participants.

## Study (MO)

We used different scanners which is not the best method either since all machines are slightly different and fMRI data is highly sensitive to difference. As most variance come from the scanners and scanning procedure (Biberacher et al., 2016) it can be hard to add the results together. All the experiments were done in a somewhat chaotic at least different manner each time. Some of the native Danish participants reported back that they thought some words were scored oddly. What makes "sandpaper" negative and "pineapple" positive? The participants had different opinions and as authors we address this once again as information loss. Binder et al. (2016) had 65 factors to explain the valence of a word. By summarizing the words 65 scores into one, we lose a lot of information and get a mean valence score for each word. Depending on participants individual experience and wiring they will perceive it differently as they must provide the context themselves. What makes "policeman" negative is most likely different from what makes "commander" negative, and the difference would really depend on the context. As a means of this study the word scores are summarized and validated using another corpus of word valence scores. If it was to capture all individual differences this study would have a different agenda. Keeping to the generalizability of the study's stimuli it is as good as it gets to accommodate several backgrounds and purposes.

The faces stimuli were not validated to whether the face is perceived as negative and positive or whether it is more negative and neutral. This could make a difference for how the analysis should be approached, as if one of the faces was a baseline an only reflecting the perceived valence of the words rather than the valence of word and the valence of the face. This would call for a different interpretation, as to the positive emotion processing and face processing. The participants could have learned from seeing the first negative face to answer "positive" when seeing the other face and not paying attention to the words, as the response was always after the face stimulus. This would however only be a problem if we expected the participants accuracy to play a role, and as we are only interested in the perceiving of valanced faces it would not cloud our analysis that much.

### Future (SK)

All in all this model was not informed enough, we do need more like it (Smaldino, 2017). Smaldino argues that even though models are stupid like assuming that the activation pattern is only predicted by valanced face stimulus rather than including the words valence or a behavioural measure, it is these models that get us thinking and make us wiser. In the previous student paper the author made directed acyclic graphs to better approximate the areas of interesting activation, a case of progression in from a simple model to a more complicated model (Fyhn Sørensen, 2022). To accommodate these points of discussions we propose a different setup to investigate the difference in processing valanced stimuli. A whole other model would be to choose a different method as for example EEG. With EEG the analysis could focus on the N170 component for face recognition and whether valanced stimulus can cause a drift in the N170 component (Blau et al., 2007; Hinojosa et al., 2015) e.g., will negative stimulus be recognized earlier than positive stimulus. It is still a question of the difference in processing of valanced stimuli, just a more temporal angle, where the areas of interest do not play as crucial a role. This might provide further information of valanced stimuli processing.

## Conclusion (MO)

A pseudo-forced task was completed to investigate the relationship of brain activation during processing of valanced visual stimuli. We found brain activation patterns and trained a classification model on different contrasts. The models failed accurately predict test data. Limitations and other approaches were discussed.

## Acknowledgements

We would like to acknowledge Line Kruse's generous help with understanding and assisting in the coding process and finding Mikkel Wallentin and Lukas Snoek's tutorials on SearchLight.

We acknowledge the python software provider, such that we could run this fMRI analysis and classification on a larger scale with the UCloud interactive HPC system, managed by eScience Center at the University of Southern Denmark

## References

Abraham, A., Pedregosa, F., Eickenberg, M., Gervais, P., Mueller, A., Kossaifi, J., Gramfort, A., Thirion, B., & Varoquaux, G. (2014). Machine learning for neuroimaging with scikit-learn. *Frontiers in Neuroinformatics*, *8*. https://www.frontiersin.org/articles/10.3389/fninf.2014.00014

Altman, N. S. (1992). An Introduction to Kernel and Nearest-Neighbor Nonparametric Regression. *The American Statistician*, *46*(3), 175–185. https://doi.org/10.2307/2685209

Al-Zubaidi, A., Mertins, A., Heldmann, M., Jauch-Chara, K., & Münte, T. F. (2019). Machine Learning Based Classification of Resting-State fMRI Features Exemplified by Metabolic State (Hunger/Satiety). *Frontiers in Human Neuroscience*, *13*. https://www.frontiersin.org/articles/10.3389/fnhum.2019.00164

Amaro, E., & Barker, G. J. (2006). Study design in fMRI: Basic principles. *Brain and Cognition*, *60*(3), 220–232. https://doi.org/10.1016/j.bandc.2005.11.009

Barrett, L. F. (2006). Are Emotions Natural Kinds? *Perspectives on Psychological Science*, *1*(1), 28–58. https://doi.org/10.1111/j.1745-6916.2006.00003.x

Bear, M. F., Connors, B. W., & Paradiso, M. A. (2016). *Neuroscience: Exploring the Brain* (4th ed.). Jones & Bartlett Learning.

Berwick, R. C., Friederici, A. D., Chomsky, N., & Bolhuis, J. J. (2013). Evolution, brain, and the nature of language. *Trends in Cognitive Sciences*, *17*(2), 89–98. https://doi.org/10.1016/j.tics.2012.12.002

Biberacher, V., Schmidt, P., Keshavan, A., Boucard, C. C., Righart, R., Sämann, P., Preibisch, C., Fröbel, D., Aly, L., Hemmer, B., Zimmer, C., Henry, R. G., & Mühlau, M. (2016). Intra- and interscanner variability of magnetic resonance imaging based volumetry in multiple sclerosis | Elsevier Enhanced Reader. *NeuroImage*, *142*, 188–197. https://doi.org/10.1016/j.neuroimage.2016.07.035

Binder, J. R., Conant, L. L., Humphries, C. J., Fernandino, L., Simons, S. B., Aguilar, M., & Desai, R. H. (2016). Toward a brain-based componential semantic representation. *Cognitive Neuropsychology*. https://doi.org/10.1080/02643294.2016.1147426

Blau, V. C., Maurer, U., Tottenham, N., & McCandliss, B. D. (2007). The face-specific N170 component is modulated by emotional facial expression. *Behavioral and Brain Functions*, *3*, 7. https://doi.org/10.1186/1744-9081-3-7

Boyd, R., Richerson, P. J., & Henrich, J. (2011). The cultural niche: Why social learning is essential for human adaptation. *Proceedings of the National Academy of Sciences of the United States of America*, *108 Suppl 2*(Suppl 2), 10918–10925. https://doi.org/10.1073/pnas.1100290108

Buxton, R. B. (2013). The physics of functional magnetic resonance imaging (fMRI). *Reports on Progress in Physics. Physical Society (Great Britain)*, *76*(9), 096601. https://doi.org/10.1088/0034-4885/76/9/096601

Cortes, C., & Vapnik, V. (1995). Support-vector networks. *Machine Learning*, *20*(3), 273–297. https://doi.org/10.1007/BF00994018

Ebner, N. C., Luedicke, J., Voelkle, M. C., Riediger, M., Tin, T., & Lindenberger, U. (2018). An adult developmental approach to perceived facial attractiveness and distinctiveness. *Frontiers in Psychology*, *9*, article 561. https://doi.org/10.3389/fpsyg.2018.00561

Ebner, N. C., Riediger, M., & Lindenberger, U. (2010). FACES—A database of facial expressions in young, middle-aged, and older women and men: Development and validation. *Behavior Research Methods*, *42*(1), 351–362. https://doi.org/10.3758/BRM.42.1.351

Ekman, P. (1992). An argument for basic emotions. *Cognition and Emotion*, *6*, 169–200. https://doi.org/10.1080/02699939208411068

Ekman, P. (2000). Facial expressions. In *Handbook of Cognition and Emotion* (pp. 301–319). John Wiley & Sons.

Etzel, J. A., Zacks, J. M., & Braver, T. S. (2013). Searchlight analysis: Promise, pitfalls, and potential. *NeuroImage*, *78*, 261–269. https://doi.org/10.1016/j.neuroimage.2013.03.041

Fisher, S. R. A. (1971). The Design of Experiments. *Hafner Press*, *9*, 256.

Fyhn Sørensen, S. (2022). *Sigurds exam paper for cognitive neuroscience.*

Gazzaniga, M. S., Ivry, R. B., & Mangun, G. R. (2014). *Cognitive Neuroscience: The Biology of the Mind* (4th ed.). W. W. Norton & Company.

Goldstein, E. B., & Van Hoff, J. C. (2020). *Cognitive Psychology* (2nd ed.). Cengage.

Hamann, S. (2012). Mapping discrete and dimensional emotions onto the brain: Controversies and consensus. *Trends in Cognitive Sciences*, *16*(9), 458–466. https://doi.org/10.1016/j.tics.2012.07.006

Hargreaves, B. (2012). Rapid Gradient-Echo Imaging. *Journal of Magnetic Resonance Imaging : JMRI*, *36*(6), 1300–1313. https://doi.org/10.1002/jmri.23742

Heyes, C. M., & Frith, C. D. (2014). The cultural evolution of mind reading. *Science*, *344*(6190), 1243091. https://doi.org/10.1126/science.1243091

Hinojosa, J. A., Mercado, F., & Carretié, L. (2015). N170 sensitivity to facial expression: A meta-analysis. *Neuroscience & Biobehavioral Reviews*, *55*, 498–509. https://doi.org/10.1016/j.neubiorev.2015.06.002

Holland, C. A. C., Ebner, N. C., & Lin, T. (2018). Emotion identification across adulthood using the Dynamic FACES database of emotional expressions in younger, middle aged, and older adults. *Cognition and Emotion*, *33*(2), 245–25. https://doi.org/10.1080/02699931.2018.1445981

Huettel, S. A., Song, A. W., & McCarthy. (2009). Functional Magnetic Resonance Imaging. *The Yale Journal of Biology and Medicine*, *82*(4), 233.

Kanwisher, N., McDermott, J., & Chun, M. M. (1997). The Fusiform Face Area: A Module in Human Extrastriate Cortex Specialized for Face Perception. *Journal of Neuroscience*, *17*(11), 4302–4311. https://doi.org/10.1523/JNEUROSCI.17-11-04302.1997

Kluyver, T., Ragan-Kelley, B., Pérez, F., Granger, B., Bussonnier, M., Frederic, J., Kelley, K., Hamrick, J., Grout, J., Corlay, S., Ivanov, P., Avila, D., Abdalla, S., Willing, C., & Jupyter development team. (2016). *Jupyter Notebooks – a publishing format for reproducible computational workflows* (F. Loizides & B. Scmidt, Eds.; pp. 87–90). IOS Press. https://doi.org/10.3233/978-1-61499-649-1-87

LeDoux, J. E. (1996). *The emotional brain: The mysterious underpinnings of emotional life* (p. 384). Simon & Schuster.

LeDoux, J. E. (2003). The Emotional Brain, Fear and the Amygdala. *Cellular and Molecular Neurobiology*, *23*(4/5). https://doi.org/0272-4340/03/1000-0727/0

Maclean, P. D. (1949). Psychosomatic disease and the 'visceral brain'; recent developments bearing on the Papez theory of emotion. *Psychosomatic Medicine*, *11*, 338–353. https://doi.org/10.1097/00006842-194911000-00003

Mahmoudi, A., Takerkart, S., Regragui, F., Boussaoud, D., & Brovelli, A. (2012). Multivoxel pattern analysis for FMRI data: A review. *Computational and Mathematical Methods in Medicine*, *2012*, 961257. https://doi.org/10.1155/2012/961257

Mahon, B. Z. (2022). Chapter 13—Domain-specific connectivity drives the organization of object knowledge in the brain. In G. Miceli, P. Bartolomeo, & V. Navarro (Eds.), *Handbook of Clinical Neurology* (Vol. 187, pp. 221–244). Elsevier. https://doi.org/10.1016/B978-0-12-823493-8.00028-6

Meadows, M.-E. (2011). Calcarine Cortex. In J. S. Kreutzer, J. DeLuca, & B. Caplan (Eds.), *Encyclopedia of Clinical Neuropsychology* (pp. 472–472). Springer. https://doi.org/10.1007/978-0-387-79948-3_1348

*MRI interpretation*. (n.d.). Retrieved 3 June 2023, from https://www.radiologymasterclass.co.uk/tutorials/mri/mri_signal

Notter, M., Gale, D., Herholz, P., Markello, R., Notter-Bielser, M.-L., & Whitaker, K. (2019). AtlasReader: A Python package to generate coordinate tables, region labels, and informative figures from statistical MRI images. *Journal of Open Source Software*, *4*(34), 1257. https://doi.org/10.21105/joss.01257

Papez, J. W. (1937). A PROPOSED MECHANISM OF EMOTION. *Archives of Neurology & Psychiatry*, *38*(4), 725–743. https://doi.org/10.1001/archneurpsyc.1937.02260220069003

Pitman, E. J. G. (1937). Significance Tests Which May be Applied to Samples from any Populations. II. The Correlation Coefficient Test. *Supplement to the Journal of the Royal Statistical Society*, *4*(2), 225–232. https://doi.org/10.2307/2983647

Posit team. (2023). *Rstudio: Integrated Development Environment for R*. Posit Software, PBC. http://www.posit.co/

Posner, M. I., & Raichle, M. E. (1994). *Images of mind* (pp. ix, 257). Scientific American Library/Scientific American Books.

R Core Team. (2022). *R: A language and environment for statistical computing*. https://www.R-project.org/.

Raju, H., & Tadi, P. (2023). Neuroanatomy, Somatosensory Cortex. In *StatPearls*. StatPearls Publishing. http://www.ncbi.nlm.nih.gov/books/NBK555915/

Schölvinck, M. L., Howarth, C., & Attwell, D. (2008). The cortical energy needed for conscious perception. *Neuroimage*, *40*(4), 1460–1468. https://doi.org/10.1016/j.neuroimage.2008.01.032

Schupp, H. T., Flaisch, T., Stockburger, J., & Junghöfer, M. (2006). Emotion and attention: Event-related brain potential studies. *Progress in Brain Research*, *156*, 31–51. https://doi.org/10.1016/S0079-6123(06)56002-9

Smaldino, P. E. (2017). Models Are Stupid, and We Need More of Them. In *Computational Social Psychology*. Routledge.

Sutton, T. M., & Lutz, C. (2019). Attentional capture for emotional words and images: The importance of valence and arousal. *Canadian Journal of Experimental Psychology = Revue Canadienne De Psychologie Experimentale*, *73*(1), 47–54. https://doi.org/10.1037/cep0000154

Tsiourti, C., Weiss, A., Wac, K., & Vincze, M. (2019). Multimodal Integration of Emotional Signals from Voice, Body, and Context: Effects of (In)Congruence on Emotion Recognition and Attitudes Towards Robots. *International Journal of Social Robotics*, *11*. https://doi.org/10.1007/s12369-019-00524-z

Van Rossum, G., & Drake, F. L. (2009). *Python 3 Reference Manual*. CreateSpace.

Ward, J. (2020). *The Student's Guide to Cognitive Neuroscience* (4th ed.). Routledge.

Warriner, A. B., Kuperman, V., & Brysbaert, M. (2013). Norms of valence, arousal, and dominance for 13,915 English lemmas. *Behavior Research Methods*, *45*(4), 1191–1207. https://doi.org/10.3758/s13428-012-0314-x

Wickham, H., Averick, M., Bryan, J., Chang, W., McGowan, L., François, R., Grolemund, G., Hayes, A., Henry, L., Hester, J., Kuhn, M., Pedersen, T., Miller, E., Bache, S., Müller, K., Ooms, J., Robinson, D., Seidel, D., Spinu, V., … Yutani, H. (2019). Welcome to the Tidyverse. *Journal of Open Source Software*, *4*(43), 1686. https://doi.org/10.21105/joss.01686

Xu, Y., He, Y., & Bi, Y. (2017). A Tri-network Model of Human Semantic Processing. *Frontiers in Psychology*, *8*. https://www.frontiersin.org/articles/10.3389/fpsyg.2017.01538

# Appendices

## Appendix A: z-maps for all participants for all sessions for both conditions

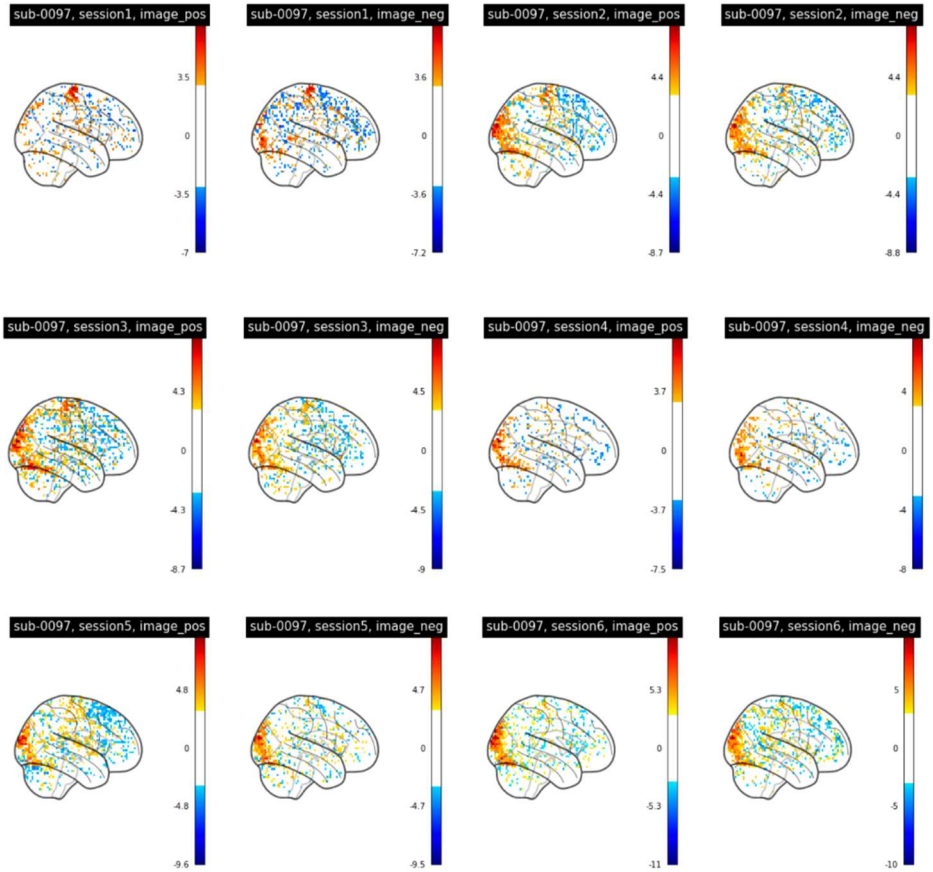


## Appendix B: second level model z-maps for Positive and Negative conditions combined

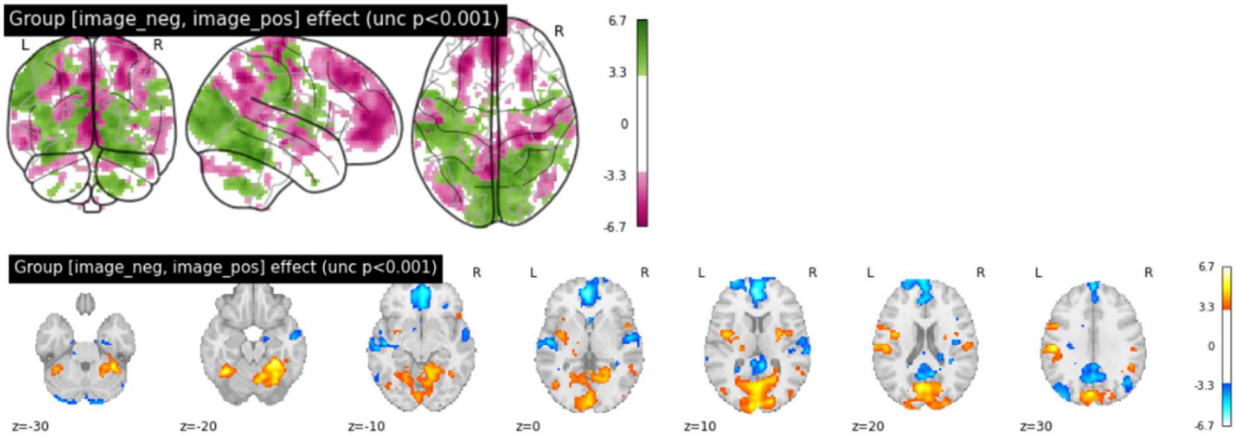


Second level model z-map for both image conditions compared to baseline activity with uncorrected p-value threshold.

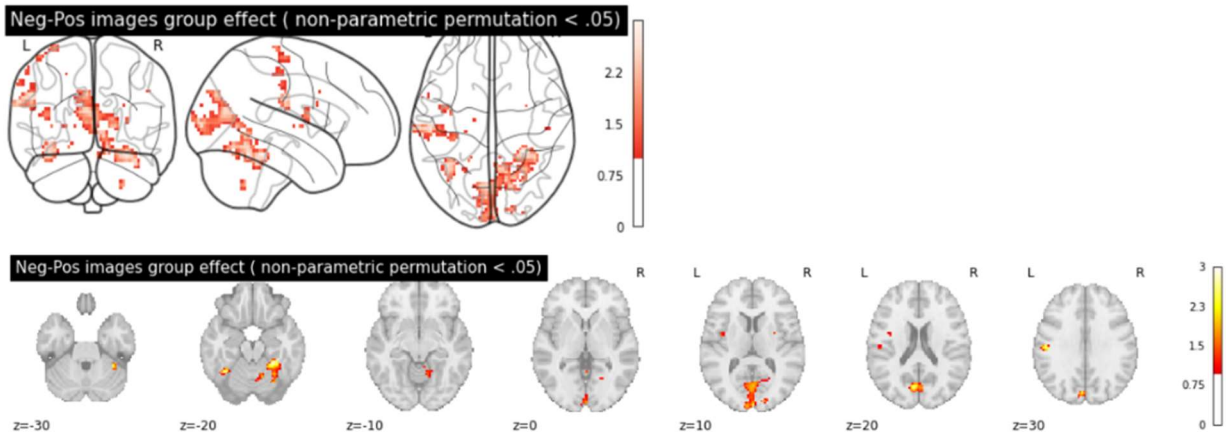


Second level model z-map for both image conditions compared to baseline activity with corrected p-value threshold based on permutation test.

## Appendix C: Atlas'

| cluster_id | peak_x | peak_y | peak_z | peak_value | volume_mm | aal | desikan_killiany | harvard_oxford |
|---|---|---|---|---|---|---|---|---|
| 1 | -0.511999 | -74.402 | 0.539999 | 3.00043 | 199152.0000 | Lingual_L | Unknown | 72.0% Left_Lingual_Gyrus; 12.0% Right_Lingual_Gyrus; 5.0% ... |
| 2 | -45.980000 | -28.934 | 49.180000 | 3.00043 | 41742.9000 | Postcentral_L | ctx-lh-postcentral | 42.0% Left_Postcentral_Gyrus; 11.0% Left_Supramarginal_Gyr... |
| 3 | -40.928000 | -6.200 | 9.660000 | 3.00043 | 8961.5300 | Rolandic_Oper_L | Unknown | 44.0% Left_Insular_Cortex; 30.0% Left_Central_Opercular_Cor... |
| 4 | -5.564000 | 1.378 | 40.060000 | 3.00043 | 4112.2200 | Cingulate_Mid_L | ctx-lh-posteriorcingulate | 53.0% Left_Cingulate_Gyrus_anterior_division; 13.0% Left_Ju... |
| 5 | 39.904000 | 1.378 | 9.660000 | 3.00043 | 3704.8800 | Insula_R | Unknown | 51.0% Right_Insular_Cortex; 29.0% Right_Central_Opercular_... |
| 6 | 60.112000 | -36.512 | 24.860000 | 3.00043 | 2521.6400 | SupraMarginal_R | Right-Cerebral-White-Matter | 32.0% Right_Supramarginal_Gyrus_posterior_division; 16.0%... |
| 7 | -33.350000 | -56.720 | -54.180000 | 3.00043 | 1512.9900 | Cerebelum_8_L | Left-Cerebellum-Cortex | 0% no_label |
| 8 | -63.662000 | 3.904 | 27.900000 | 3.00043 | 853.4790 | no_label | Unknown | 0% no_label |
| 9 | -20.720000 | -28.934 | 0.539999 | 2.39837 | 601.3150 | Thalamus_L | Left-Thalamus-Proper | 54.0% Left_Thalamus |
| 10 | 29.800000 | -59.246 | 52.220000 | 1.63871 | 504.3290 | Angular_R | ctx-rh-superiorparietal | 42.0% Right_Lateral_Occipital_Cortex_superior_division; 15.0... |
| 11 | 29.800000 | 41.794 | 24.860000 | 2.22228 | 290.9590 | Frontal_Sup_2_R | Unknown | 66.0% Right_Frontal_Pole; 7.0% Right_Middle_Frontal_Gyrus |
| 12 | 60.112000 | -56.720 | 3.580000 | 1.55328 | 155.1780 | Temporal_Mid_R | ctx-rh-middletemporal | 70.0% Right_Middle_Temporal_Gyrus_temporooccipital_part;... |
| 13 | 55.060000 | -16.304 | 37.020000 | 1.45637 | 116.3840 | Postcentral_R | ctx-rh-postcentral | 50.0% Right_Postcentral_Gyrus |
| 14 | 7.066000 | -36.512 | -48.100000 | 1.46896 | 116.3840 | no_label | Brain-Stem | 99.0% Brain-Stem |
| 15 | -10.616000 | -26.408 | 49.180000 | 1.72168 | 96.9863 | Paracentral_Lobule_L | Unknown | 43.0% Left_Precentral_Gyrus |

| cluster_id | peak_x | peak_y | peak_z | cluster_mean | volume_mm | aal | desikan_killiany | harvard_oxford |
|---|---|---|---|---|---|---|---|---|
| 1 | -3.038 | -81.980 | 12.70 | 1.51813 | 7700.710 | 52.39% Calcarine_L; 22.92% Cuneus_L; 15.62% Calcarine_R | 27.71% Left-Cerebral-White-Matter; 21.66% ctx-lh-cuneus; 1... | 20.65% Left_Intracalcarine_Cortex; 18.64% Left_Cuneal_Cort... |
| 2 | 27.274 | -41.564 | -20.74 | 1.69311 | 3413.920 | 44.89% Cerebelum_6_R; 30.11% Fusiform_R; 23.86% Cerebel... | 46.59% Right-Cerebellum-Cortex; 41.48% Unknown; 11.36%... | 54.55% Right_Temporal_Occipital_Fusiform_Cortex; 35.23% ... |
| 3 | -53.558 | -21.356 | 27.90 | 1.71457 | 1765.150 | 48.35% Postcentral_L; 40.66% SupraMarginal_L; 5.49% Pariet... | 35.16% ctx-lh-supramarginal; 28.57% Left-Cerebral-White-... | 69.23% Left_Postcentral_Gyrus; 21.98% Left_Supramarginal_... |
| 4 | 14.644 | -66.824 | -20.74 | 1.48675 | 1687.560 | 42.53% Cerebelum_6_R; 28.74% Lingual_R; 17.24% Cerebelu... | 57.47% Right-Cerebellum-Cortex; 35.63% Unknown; 6.90% c... | 63.22% Right_Lingual_Gyrus; 22.99% no_label; 13.79% Right... |
| 5 | -38.402 | -54.194 | -20.74 | 1.77227 | 1590.570 | 82.93% Fusiform_L; 17.07% Cerebelum_6_L | 32.93% Unknown; 30.49% Left-Cerebral-White-Matter; 28.0... | 96.34% Left_Temporal_Occipital_Fusiform_Cortex |
| 6 | -40.928 | -1.148 | 12.70 | 1.31180 | 446.137 | 52.17% Insula_L; 47.83% Rolandic_Oper_L | 56.52% Unknown; 21.74% ctx-lh-precentral; 13.04% Left-Cer... | 82.61% Left_Central_Opercular_Cortex; 17.39% Left_Insular_... |
| 7 | -45.980 | -21.356 | 64.38 | 1.24369 | 349.151 | 72.22% Postcentral_L; 16.67% no_label; 11.11% Precentral_L | 44.44% Unknown; 33.33% ctx-lh-postcentral; 22.22% Left-Ce... | 100.00% Left_Postcentral_Gyrus |
| 8 | -58.610 | -26.408 | 52.22 | 1.14432 | 290.959 | 46.67% Parietal_Inf_L; 40.00% no_label; 13.33% Postcentral_L | 80.00% Unknown; 13.33% ctx-lh-postcentral; 6.67% Left-Cer... | 73.33% Left_Postcentral_Gyrus; 26.67% Left_Supramarginal_... |
| 9 | -33.350 | -28.934 | 73.50 | 1.41794 | 232.767 | 50.00% Postcentral_L; 25.00% Precentral_L; 25.00% no_label | 50.00% ctx-lh-postcentral; 41.67% Unknown; 8.33% Left-Cer... | 91.67% Left_Postcentral_Gyrus; 8.33% Left_Precentral_Gyrus |
| 10 | 17.170 | -92.084 | 9.66 | 1.32908 | 193.973 | 60.00% Cuneus_R; 40.00% Calcarine_R | 60.00% Right-Cerebral-White-Matter; 30.00% ctx-rh-lateralo... | 100.00% Right_Occipital_Pole |
| 11 | 27.274 | -56.720 | -48.10 | 1.50540 | 155.178 | 100.00% Cerebelum_8_R | 62.50% Right-Cerebellum-Cortex; 37.50% Right-Cerebellum... | 100.00% no_label |
| 12 | -63.662 | -23.882 | 40.06 | 1.17895 | 135.781 | 71.43% SupraMarginal_L; 28.57% no_label | 57.14% ctx-lh-supramarginal; 42.86% Unknown | 71.43% Left_Postcentral_Gyrus; 28.57% Left_Supramarginal_... |

Atlas map model output for Second level model z-map for both image conditions compared to baseline activity.